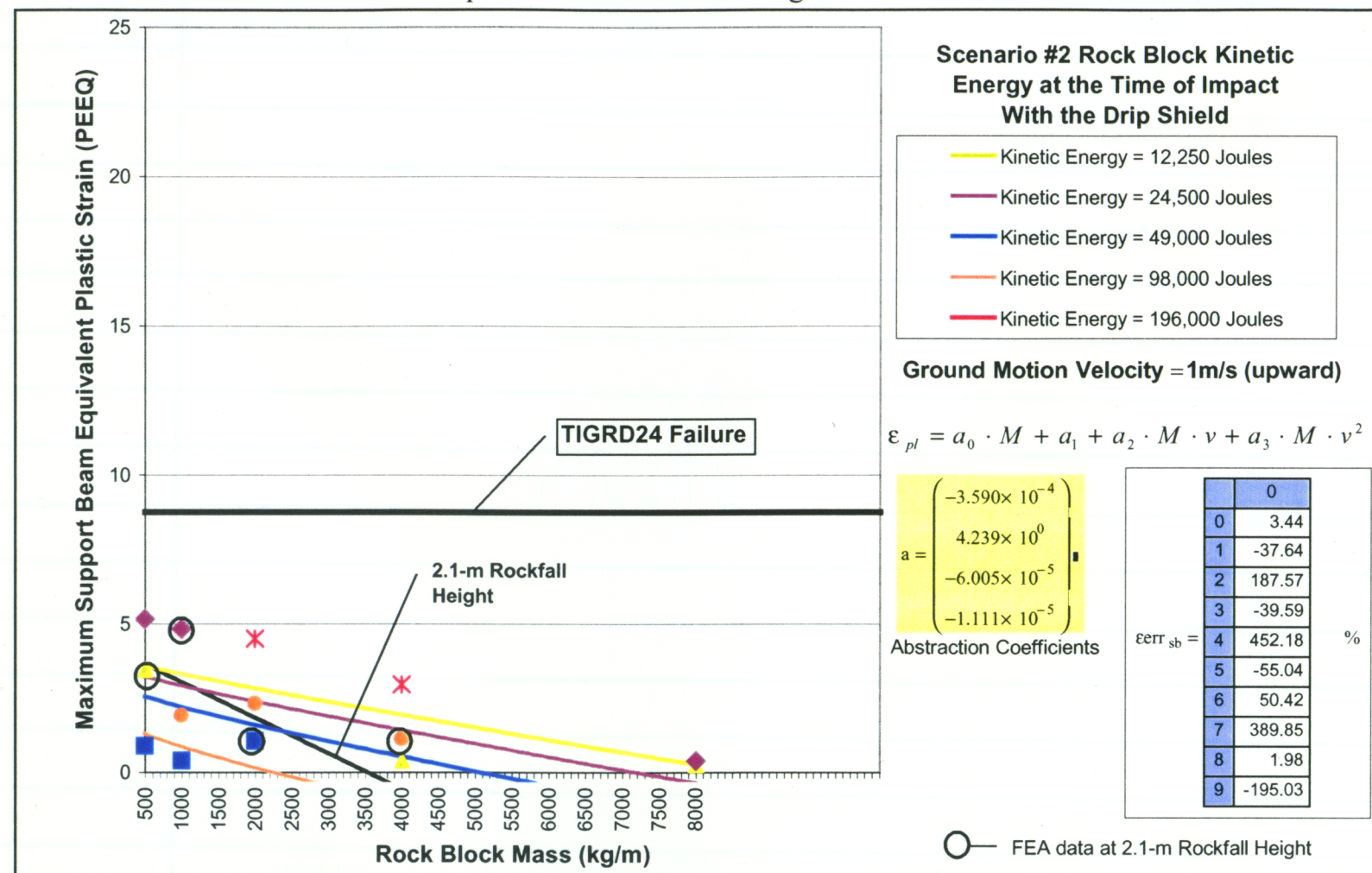
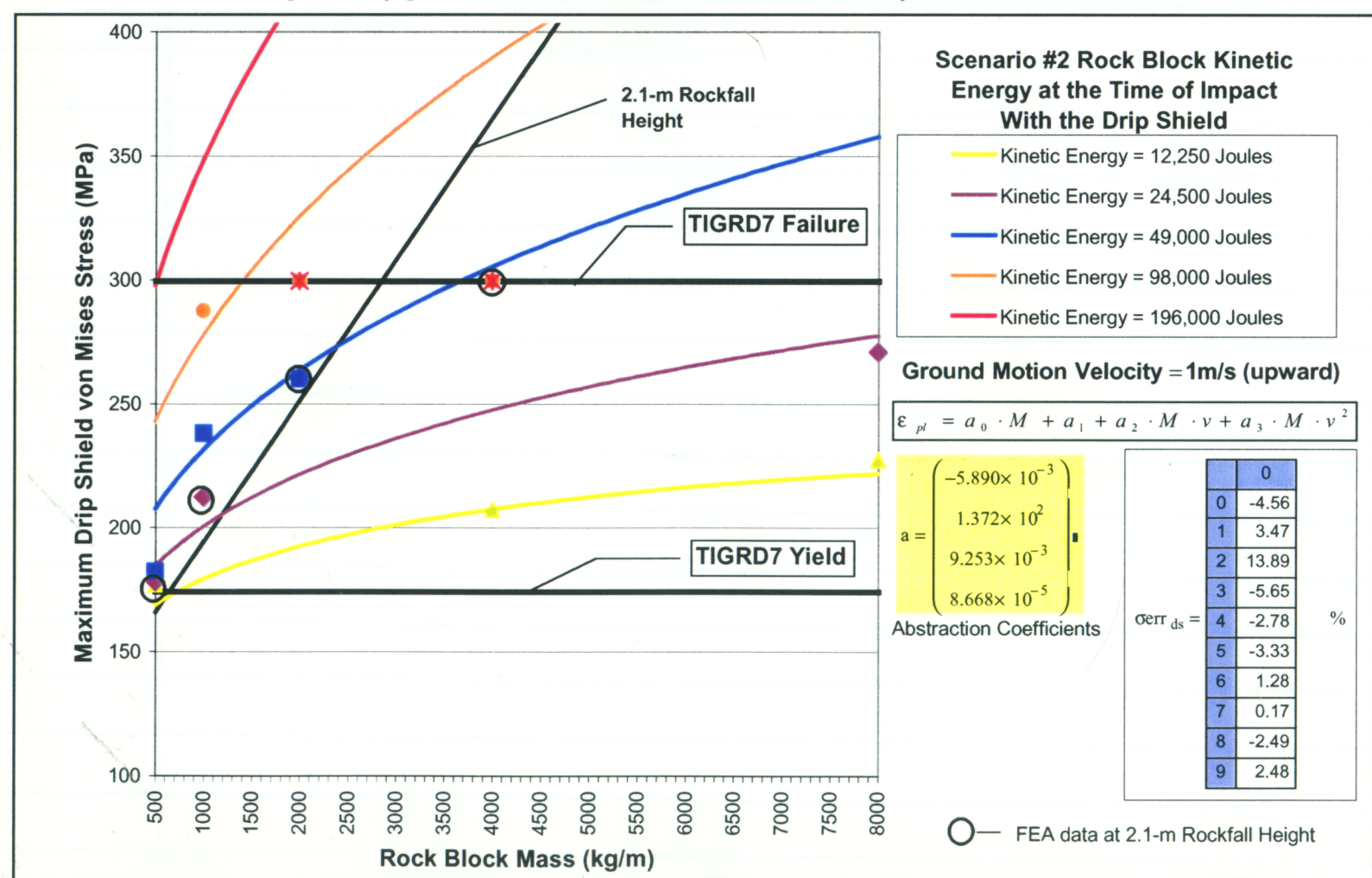


DA (4/16/02)

As noted previously, Support Beam abstractions are poor. However there is no need to track Support Beam data because failure does not occur prior to structural buckling.



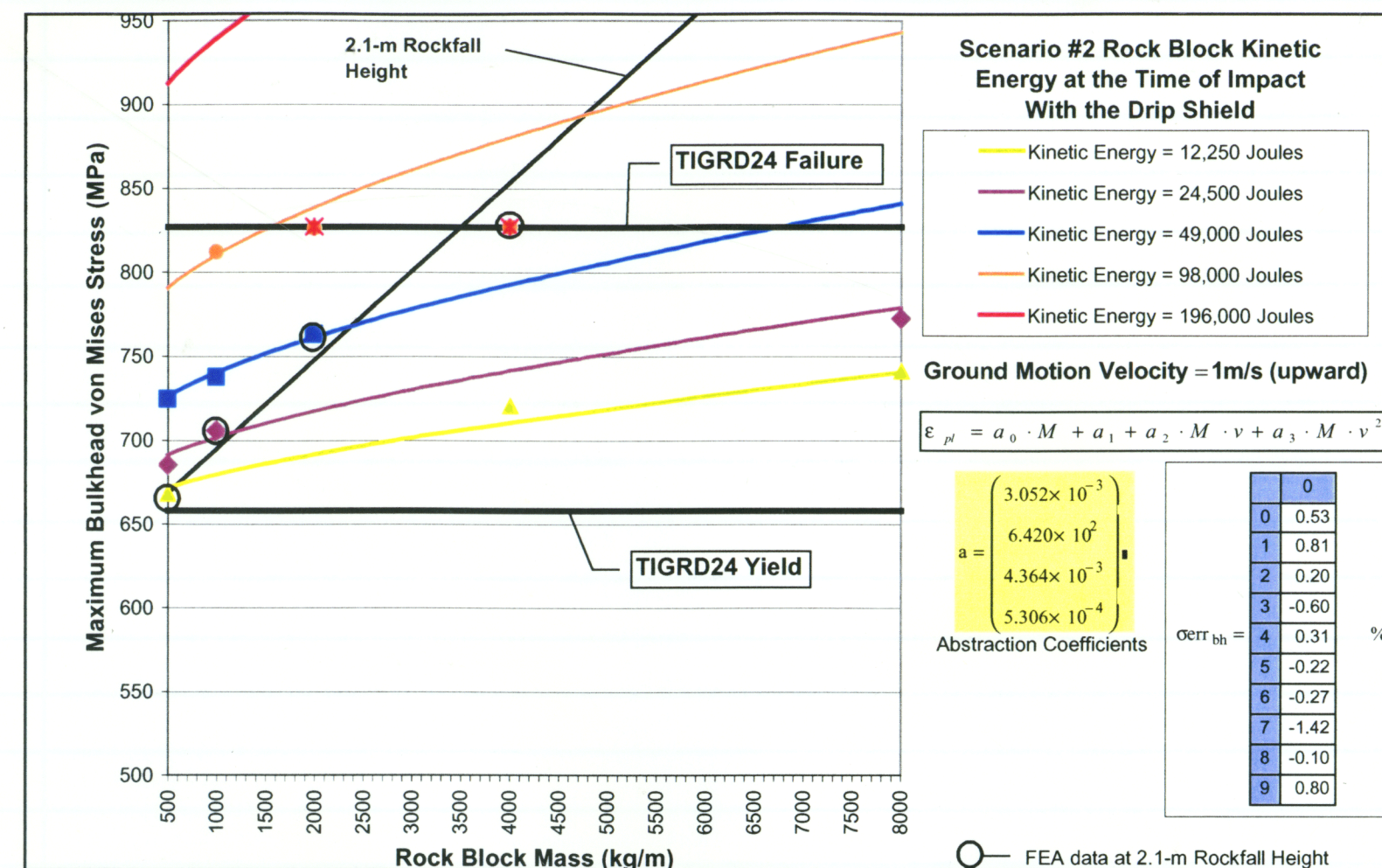
Von Mises stress abstractions for the Drip Shield and Bulkhead are very good. Predictions of the failure line are of similar quality to the PEEQ abstraction. The effect of yield stress is easy to observe in the following chart. Notice that four FE data points lie on the failure line. Once stress levels in the model exceed failure stress the behavior is perfectly plastic where the material continues to yield while stress is constant.



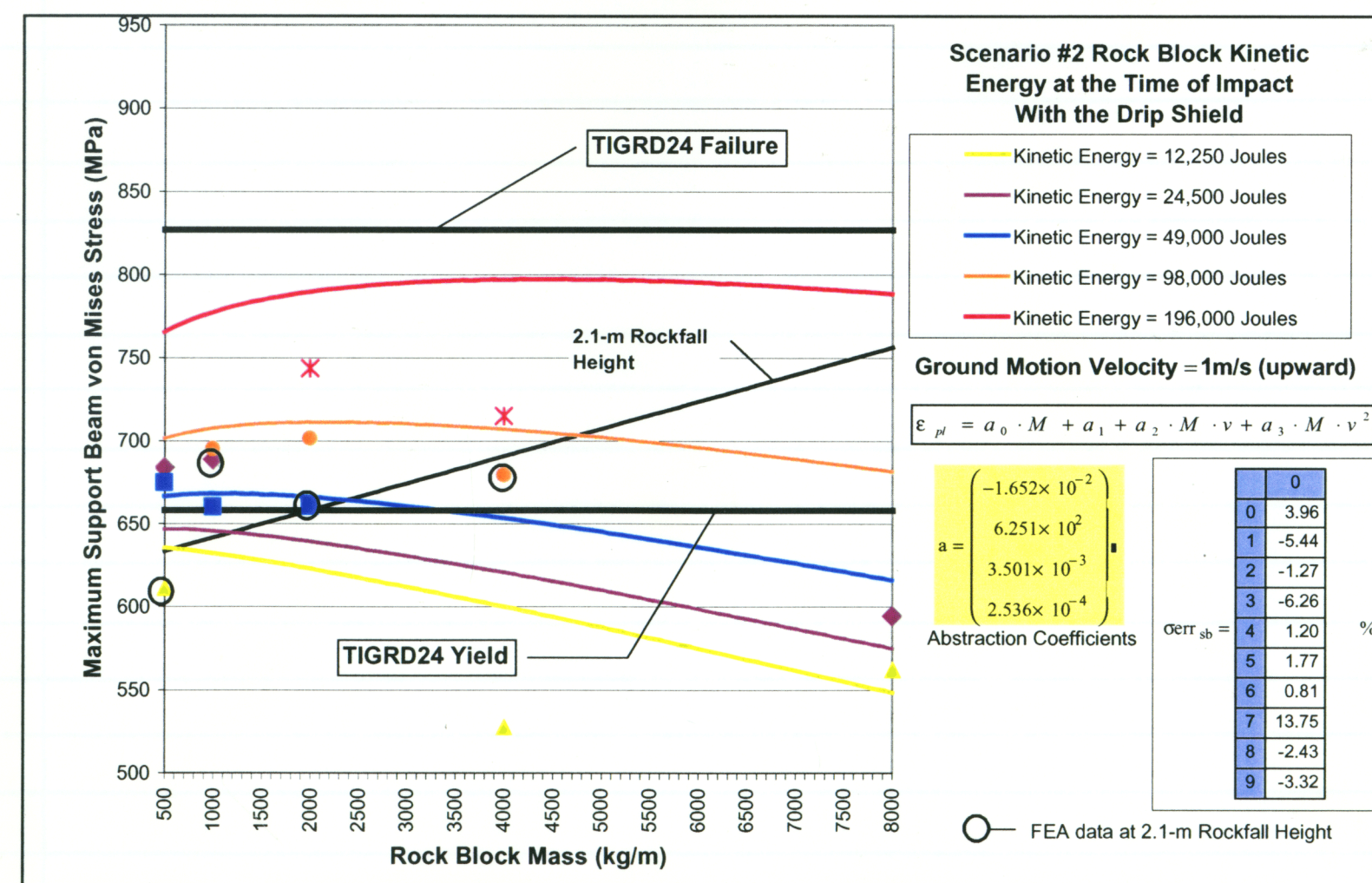
[Signature]
16 APR 2002

DA (4/16/02)

See comments on previous page.

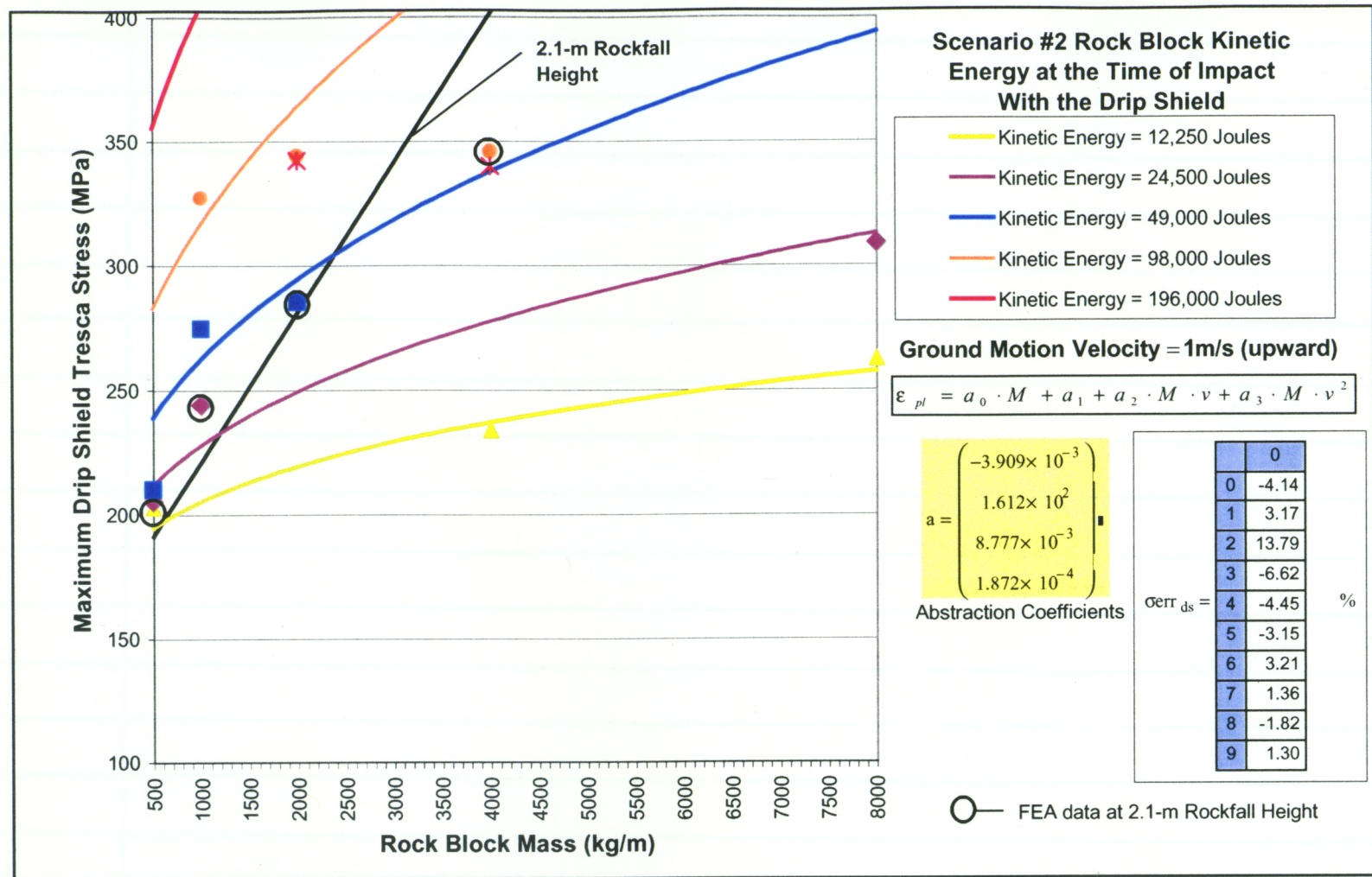


Again, the Support Beam abstraction is poor. Notice the FE data points for 2.1-m rockfall. An increase in stress is not observed with increasing rock mass as would be expected. Results appear random.

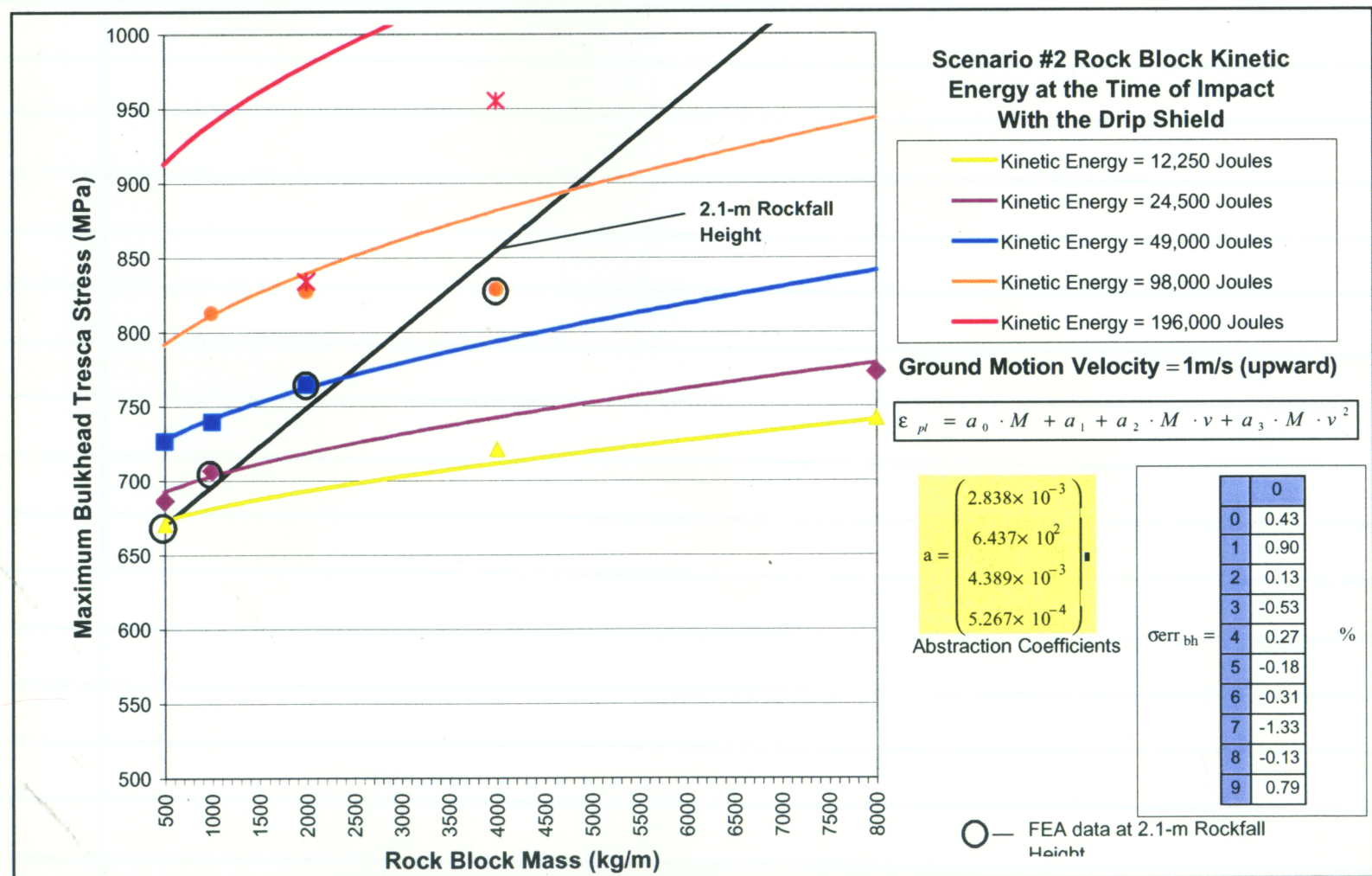


[Signature]
16 APR 2002

DA(4/16/02)



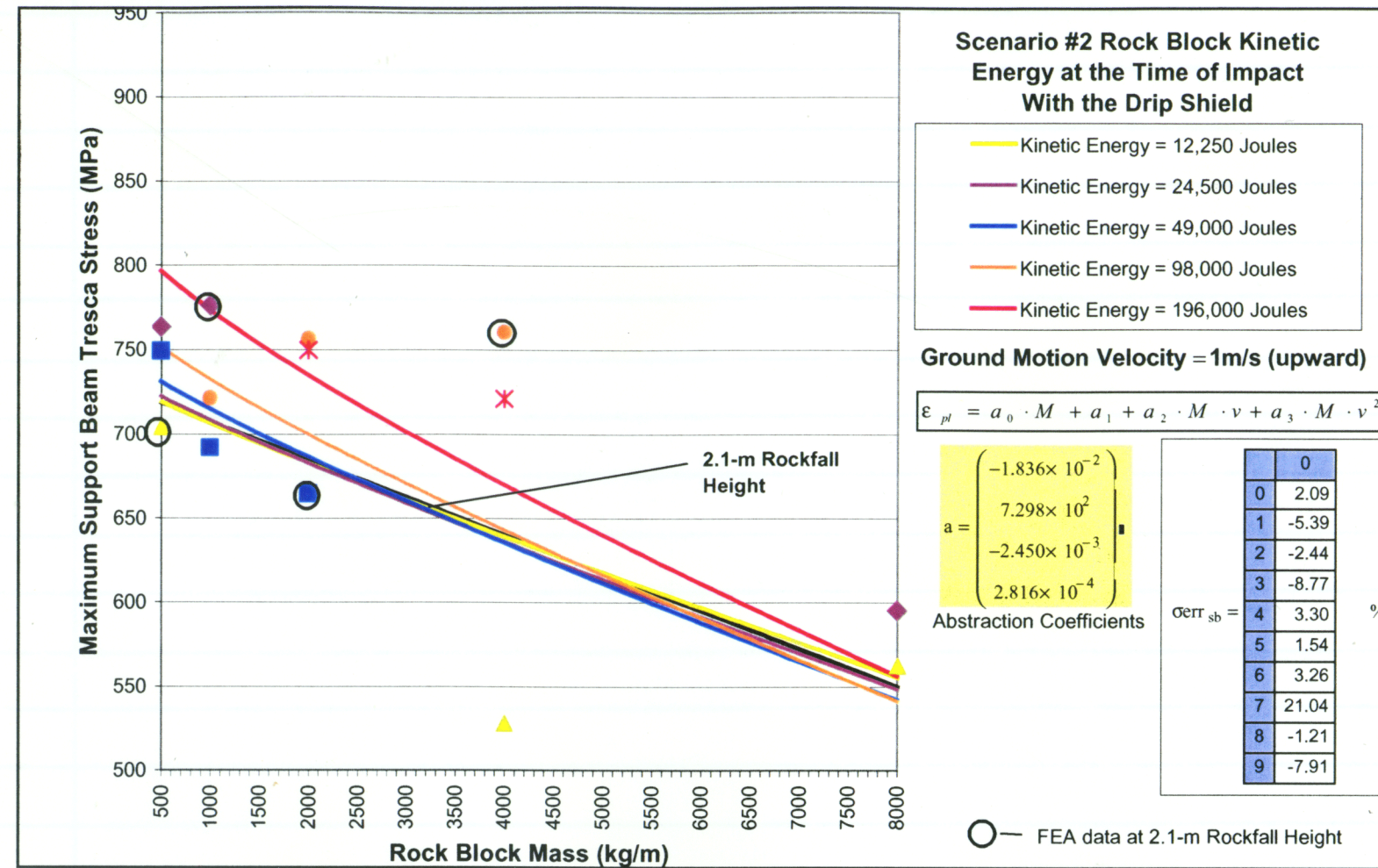
Tresca stress (max shear) abstractions for Drip Shield and Bulkhead are of similar quality to the PEEQ and von Mises stress abstractions.



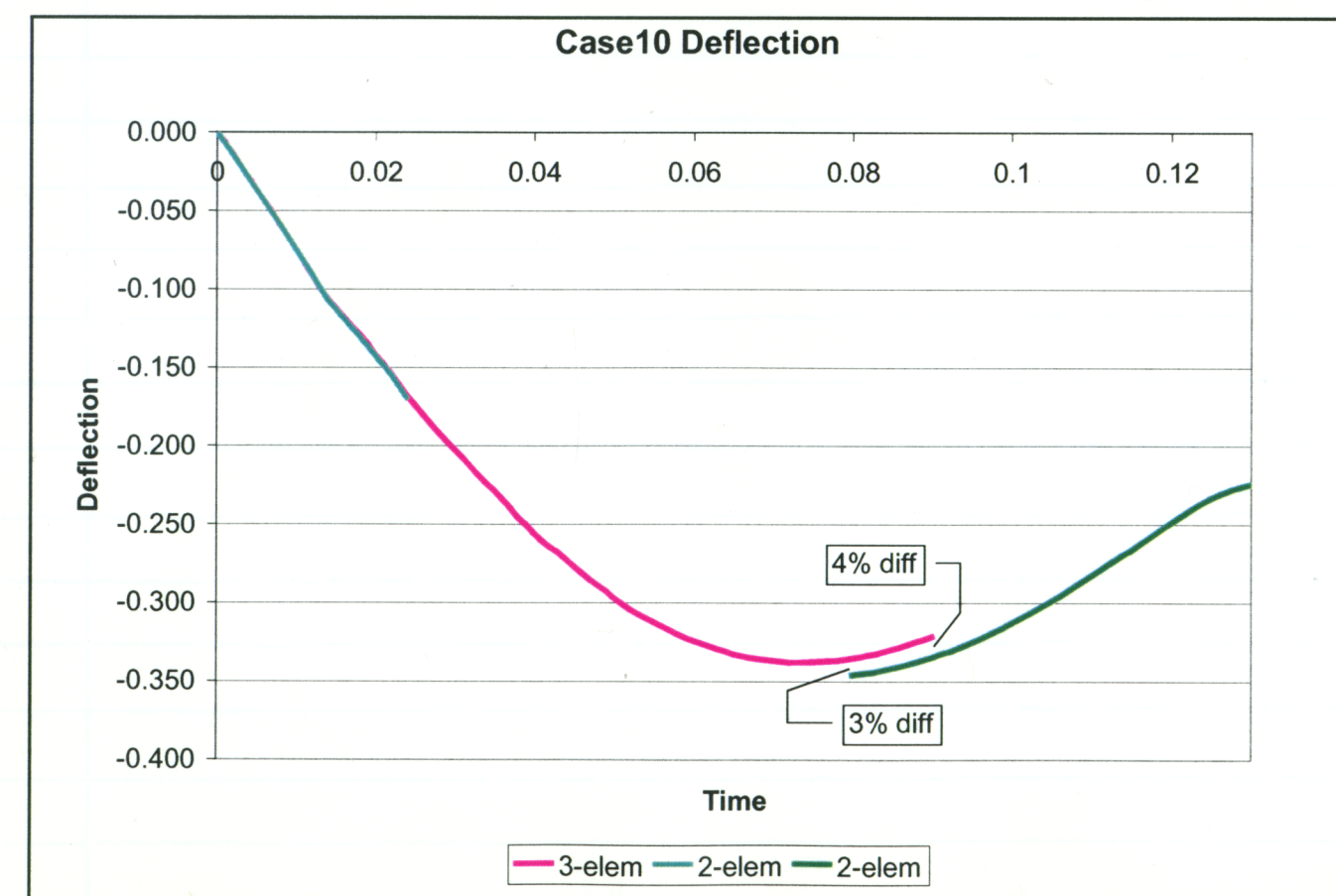
16 APR 2002

DA(4/16/02)

Again, the Support Beam abstraction is poor due to inconsistent results.



An updated finite element model was created to evaluate the significance of element density through the thickness of the Drip Shield Plate. Specifically, the model was modified to increase the number of elements through the thickness from two (2) to three (3). The Case10 load condition (as defined on page 84 of this scientific notebook) was compared. Deflection results were similar as illustrated in the figure below. The two (2) element through the thickness models are considered adequate for ABAQUS/Explicit simulations because error is less than 5% and results are conservative when compared to simulations with three (3) elements through the thickness.

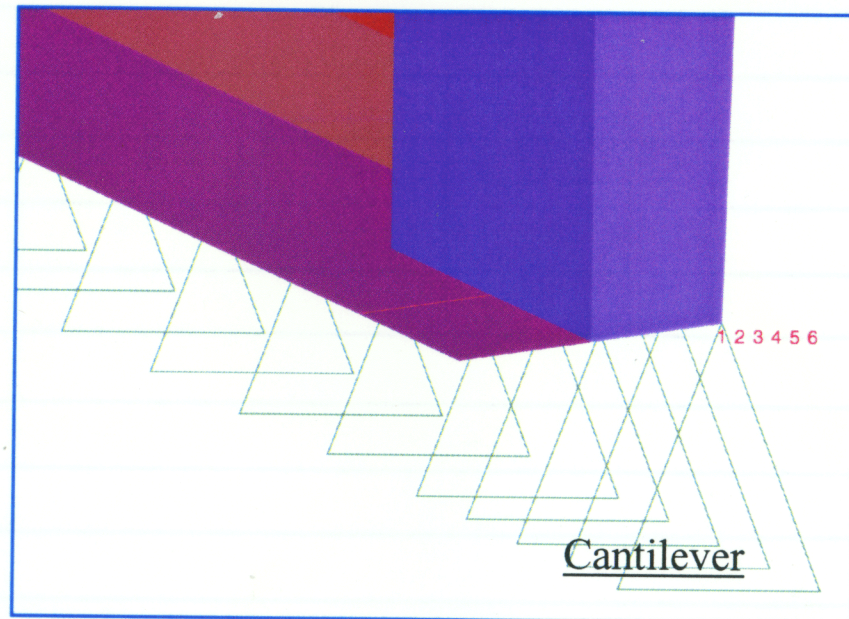
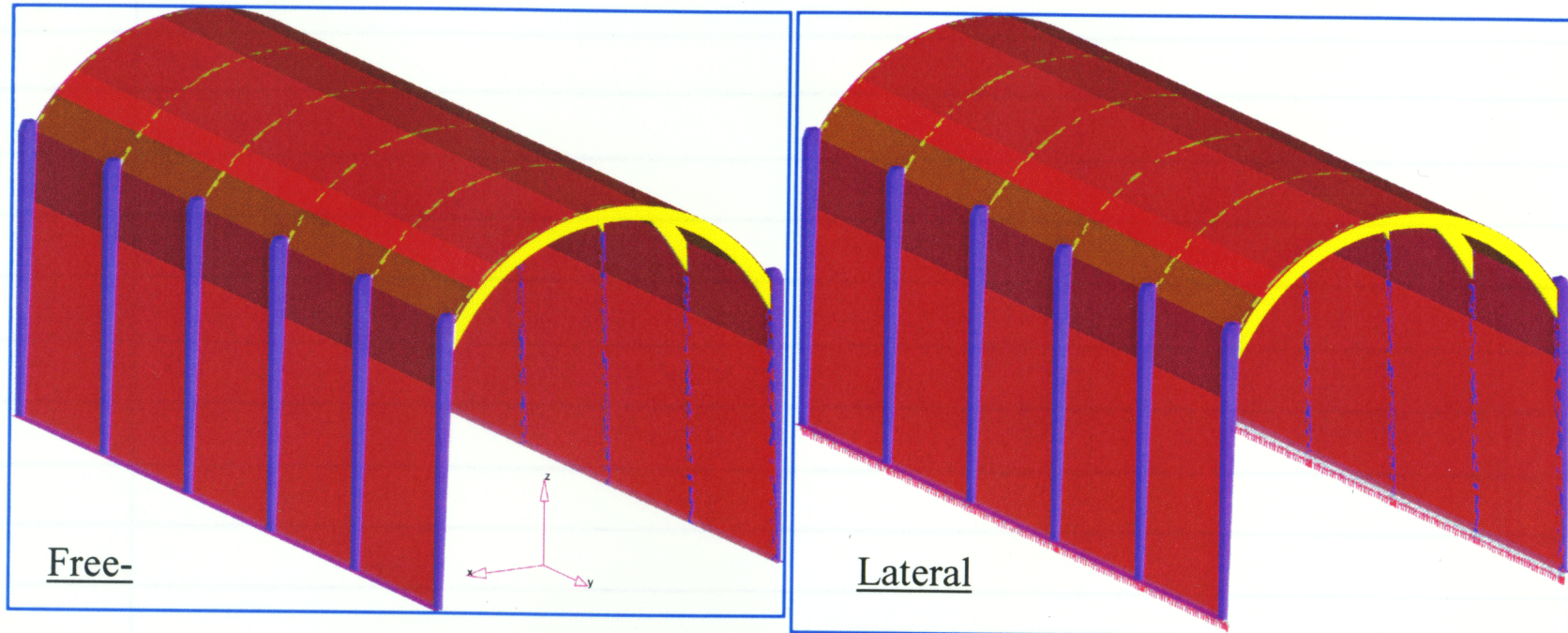


16 APR 2002

QJ (4/16/02)

SUMMARY OF MODAL ANALYSIS OF DRIP SHIELD

Analyses were performed using ABAQUS/Standard Version 5.8-16. Verification of this software is documented in the vendor's (Hibbitt, Karlsson & Sorensen, Inc.) quality program. The figures below illustrate the model and the boundary conditions used.



Free-Free boundary condition represents a completely unconstrained system.

Lateral boundary condition represents a condition where guide rails constrain lateral (side-to-side) motion of the drip shield base while axial and vertical motion remains free. There are no rotation constraints in the Lateral boundary condition. Shown above as a '1' constraint.

Cantilever boundary conditions represent a completely constrained inner edge of the drip shield base. This is similar to a base that is bolted or clamped to floor. Shown above as '123456' constraints.

[Handwritten signature]
16 APR 2002

QJ (4/16/02)

The solution was performed in four steps, each representing a separate boundary condition described above. Basic model statistics from the solution include:

NUMBER OF ELEMENTS IS 37812
 NUMBER OF NODES IS 40795
 NUMBER OF NODES DEFINED BY THE USER 40795
 TOTAL NUMBER OF VARIABLES IN THE MODEL 214260

JOB TIME SUMMARY
 USER TIME (SEC) = 9535.0
 SYSTEM TIME (SEC) = 1903.1
 TOTAL CPU TIME (SEC) = 11438.
 WALLCLOCK TIME (SEC) = 15125

Model files and results data is backed up to an 8mm tape labeled:

DRIP SHIELDS MODAL ANALYSIS
 ARCHIVED: 01 MAR 2002 TAPE 1/1

Additional data has been stored to CDROM in the directory 'DSModalAnalysis'.

The table below summarizes and compares the mode shapes and frequencies for each boundary condition described above: 'Mode' indicates the mode order sorted by frequency.

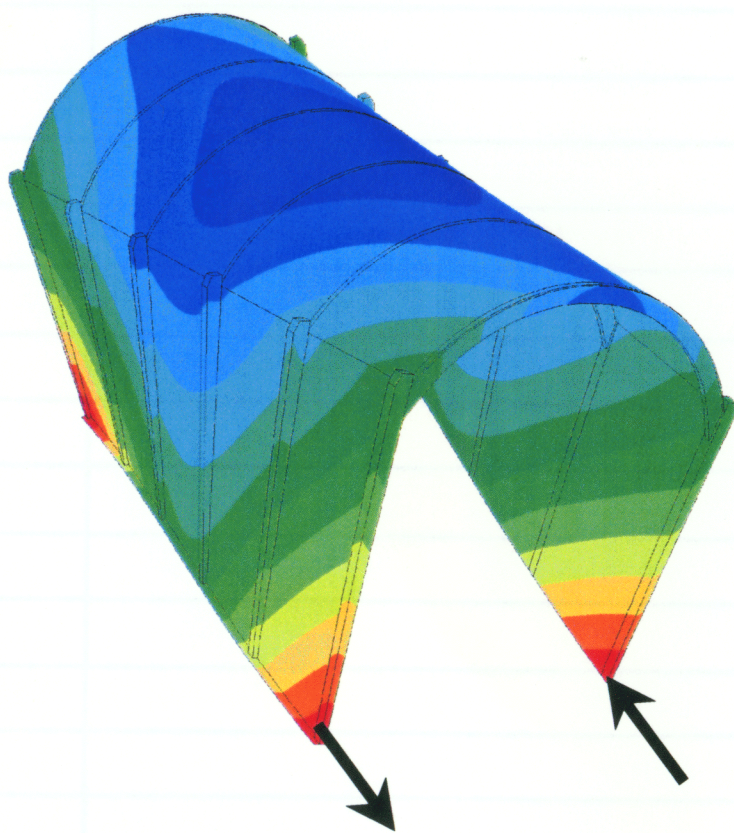
Shape	Free					Lateral					Cantilever				
	Mode	Hz	Px	Py	Pz	Mode	Hz	Px	Py	Pz	Mode	Hz	Px	Py	Pz
Free Modes	1-6	0				1-4	0				0	0			
Walking	7	2.5	4.7E-10	8.4E-12	3.3E-10	5	1.5	7.7E-10	-9.1E-10	6.8E-10					
Walk with twist one						7	9.1	1.3E-10	-4.4E-12	-3.3E-11	1	6.5	1.2E+00	-2.2E-13	-1.1E-03
Vertical up/down						6	8.7	5.1E-01	-2.3E-12	2.8E-11					
Flapping Zero	8	5.9	-1.6E-09	4.7E-12	-4.5E-11										
Flapping One	9	7.2	-1.3E-12	6.2E-11	5.8E-12										
Flapping Two	10	15.4	-1.7E-10	8.9E-12	-2.9E-11										
Flapping Three	14	23.1	-1.9E-11	1.7E-12	4.0E-13										
Flapping Four	18	34.5	-2.0E-11	-1.2E-12	3.0E-12										
Lateral Wall Zero															
Lateral Wall One						10	37.7	6.6E-01	1.2E-12	-3.3E-12	2	7.3	1.0E-04	-5.0E-11	-3.7E-01
Lateral Wall Two - mid	11	14.6	-1.4E-10	5.7E-12	7.0E-13	11	39.0	7.6E-02	-3.0E-13	-2.5E-13	5	46.7	8.9E-01	1.5E-07	2.9E-02
Lateral Wall Two - mid	12	16.2	-2.3E-10	3.7E-12	-2.3E-11	12	39.4	1.5E-09	-1.4E-12	-2.7E-13					
Lateral Wall Two - end	13	16.6	3.6E-11	-4.3E-12	-3.5E-12	13	40.0	5.5E-01	-7.1E-13	-6.9E-13					
Lateral Wall Three	15	23.5	5.6E-12	4.1E-12	1.2E-12	14	45.4	-2.2E-07	8.8E-13	-2.4E-13					
Lateral Wall Four - mid	17	33.9	5.1E-12	6.6E-13	-4.3E-13										
Lateral Wall Five - mid	20	45.1	-1.6E-12	3.5E-14	5.3E-13										
Pinch Dome Zero	16	31.6	-6.4E-11	-1.9E-12	5.7E-12	8	21.9	-2.3E-04	1.5E-12	-5.9E-12	3	26.7	-4.0E-11	-1.6E-01	-1.1E-11
Pinch Dome One	19	34.8	9.3E-12	3.9E-12	1.7E-12	9	23.8	-3.7E-12	7.2E-12	-1.7E-12	4	28.6	-1.1E-08	-7.4E-03	1.7E-08

Px, Py and Pz are the modal participation factors, which indicate the strength of motion of the subject mode shape in each of the principal directions. This is to say that a large Py (around one) indicates that an excitation in the Y-direction would likely result in large deformations of the referenced mode shape. In contrast, a low Pz (approaching zero) would indicate that an excitation in the Z-direction would result in a small deformation of the reference mode shape. Modes with high participation factors also have a potential for high stress due to a dynamic event. Significant factors are highlighted in the table above. Participation factors are not normalized to unity or necessarily greater than zero

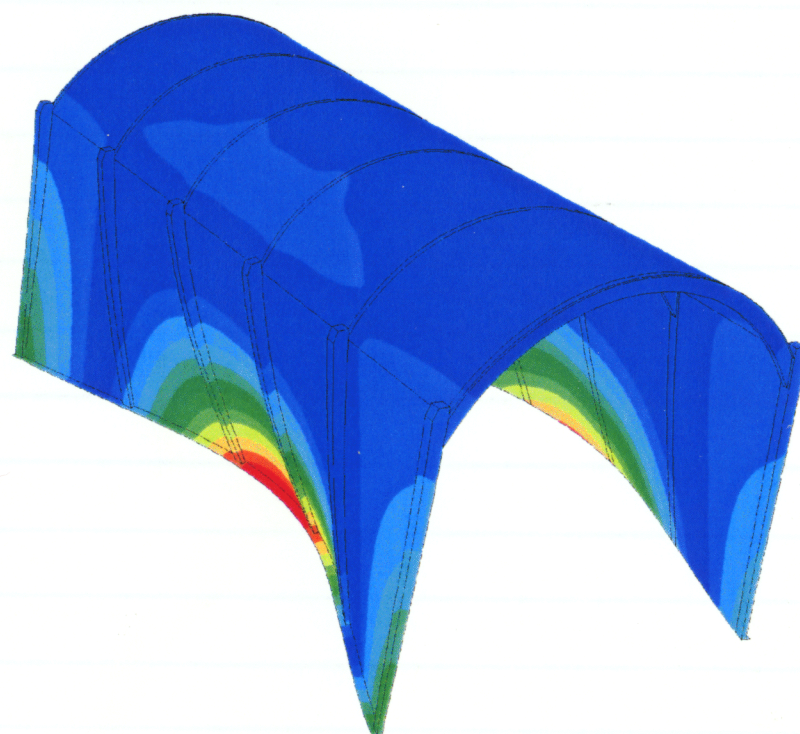
[Handwritten signature]
16 APR 2002

The following figures illustrate the major mode shapes listed in the previous table.

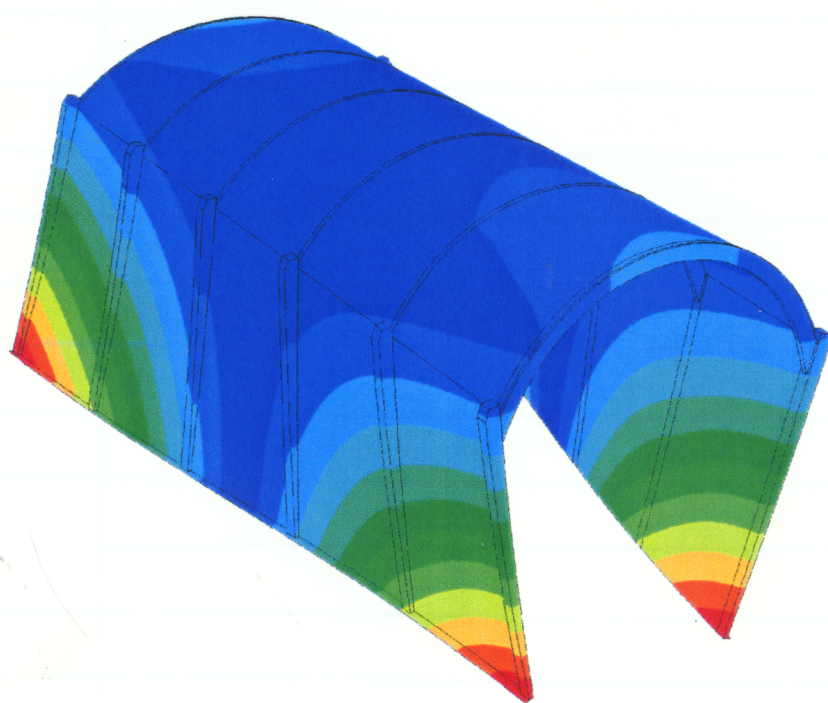
DA (4/16/02)



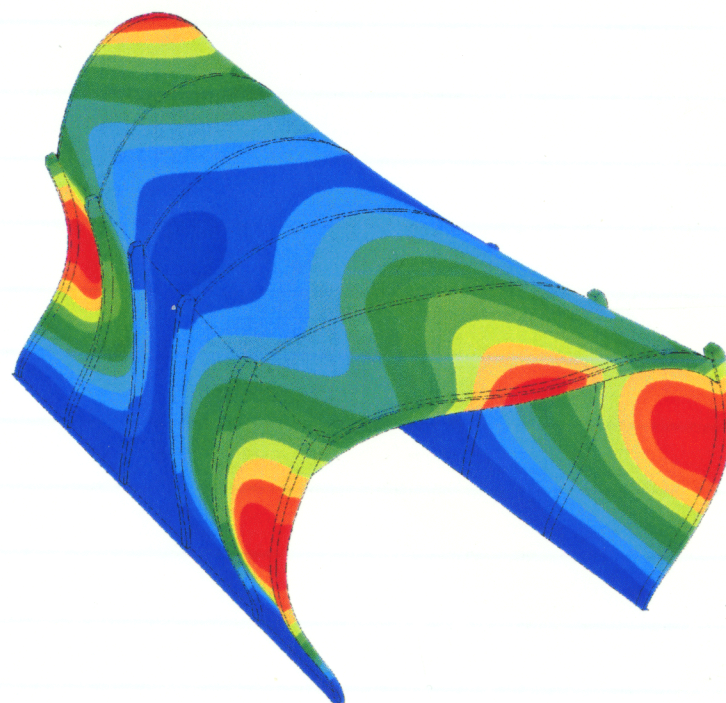
Walking is characterized by the left and right sides of the drip shield moving forward on the right and aft on the left and vice versa.



Lateral modes are characterized by opposite walls of the drip shield moving together in the lateral direction. Lateral Zero would have no shape to the wall so that it remains flat as it moves. Lateral One would have a twisting wall where on part of the wall modes in and another out. Lateral Two (shown) has additional shape to the sides. Higher orders have shapes with additional lobes.



Flapping mode shapes are similar to lateral shapes except that the opposite parts of the wall move together or away (180° out of phase). Flapping One is shown.



Pinch Dome mode shapes are characterized by the expansion and contraction (pinching) of the mid-span of the side walls. Bending of the bulkhead is also observed. Pinch Dome One is shown.

[Handwritten signature]
16 APR 2002

ESTIMATION OF DRIP SHIELD IMPACT VELOCITY WITH WASTE PACKAGE

The drip shield velocity-displacement relationship is needed to estimate the impact velocity of the drip shield with different waste package sizes in the event that the rock block impact scenario is sufficient to cause this type of interaction. The drip shield is relatively small, which indicates that a limited amount of rock block energy is absorbed by permanent deformation of the drip shield components. This is true for all cases except Case 13, which did not achieve maximum deflection and appears to be buckling. The remaining cases indicate that at maximum drip shield deflection (where velocity of the rock block is zero) the drip shield has absorbed the rock block's kinetic and potential energy primarily through elastic deformation. The deflections chart on p92 of this scientific notebook support this observation as drip shield deflection versus time follows a generally parabolic shape. Therefore, it is assumed that the drip shield and rock block interaction behaves very much like a linear elastic energy system through the point of maximum deflection.

A linear elastic energy system of equations can be solved to derive a relationship between deflection and velocity. As such the velocity of the rock block and drip shield crown when it impacts the waste package is solved by the following equation:

$$v = (v_{\text{rock}} + 1) \left[1 - \left(\frac{C}{\delta_{\text{max}}} \right)^2 \right]^{1/2}$$

where,

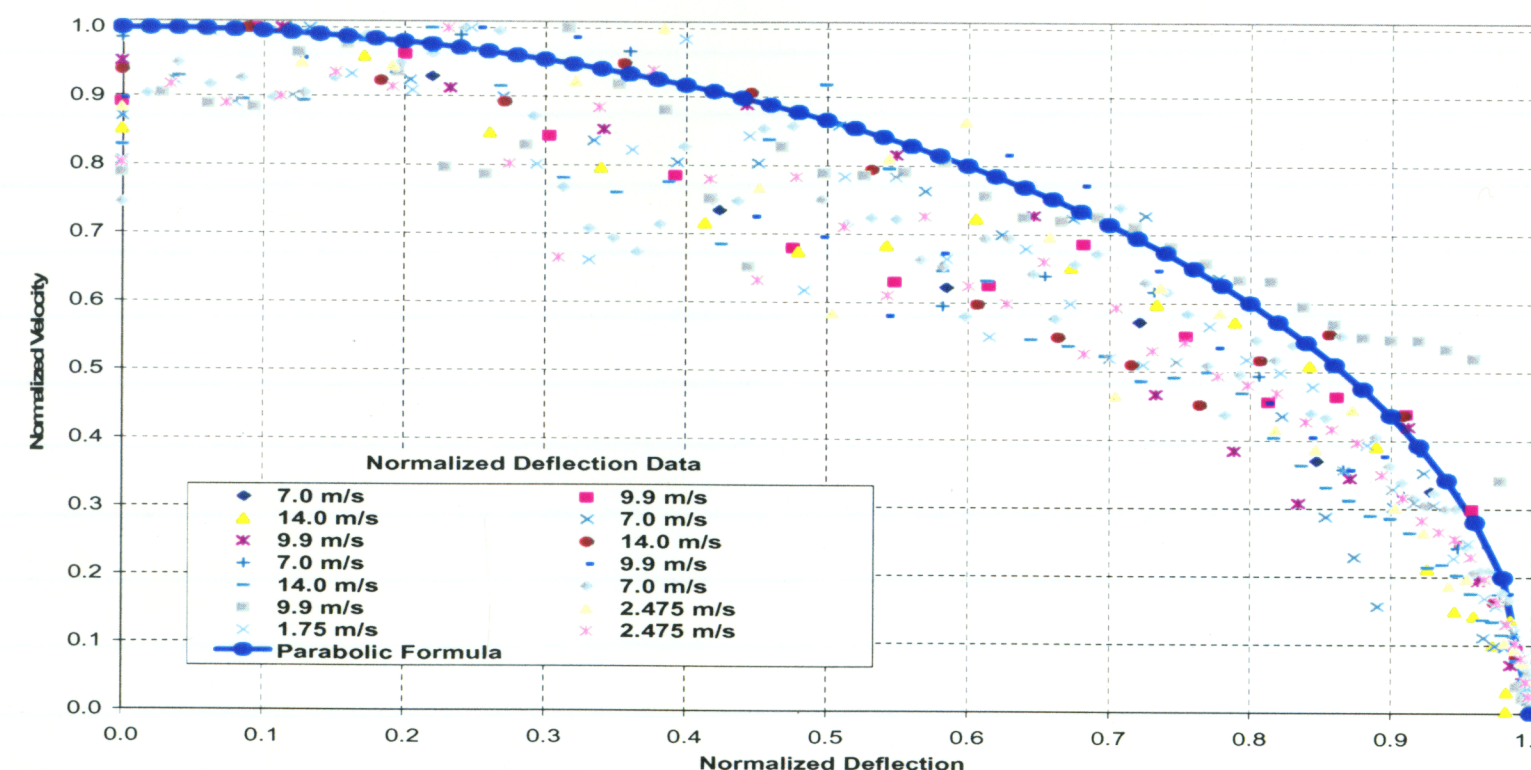
v = drip shield velocity when impacting the waste package

v_{max} = initial velocity of the rock block (at time=0)

C = clearance between drip shield and impact, C < δ_{max}

δ_{max} = maximum deflection of the drip shield if allowed to deform freely

The data points in the following figure are normalized for each scenario such that velocity and deflection have a range of zero to one. The above equation is also normalized and plotted for comparison. This data abstraction provides an excellent bounding solution to the simulation data.



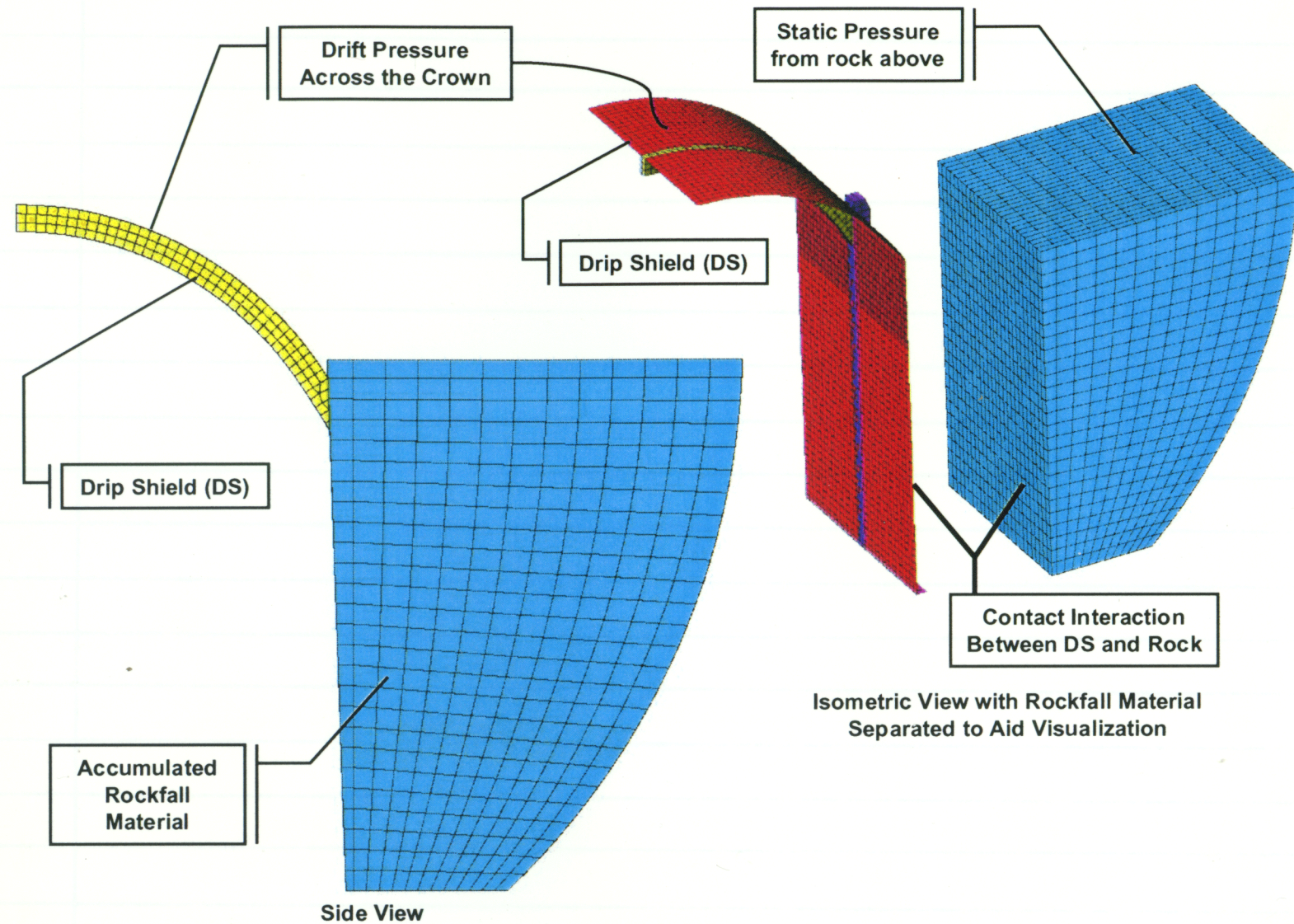
Electronic files have been archived to the CDROM labeled:

**DS and Rock Block Impact FEA
HyperMesh Models, Graphics and
Misc. Results Data Files
Nov 2002**

[Handwritten signature]
14 NOV 2002

FINITE ELEMENT ANALYSIS OF DRIP SHIELD UNDER ACCUMULATED ROCKFALL LOADS

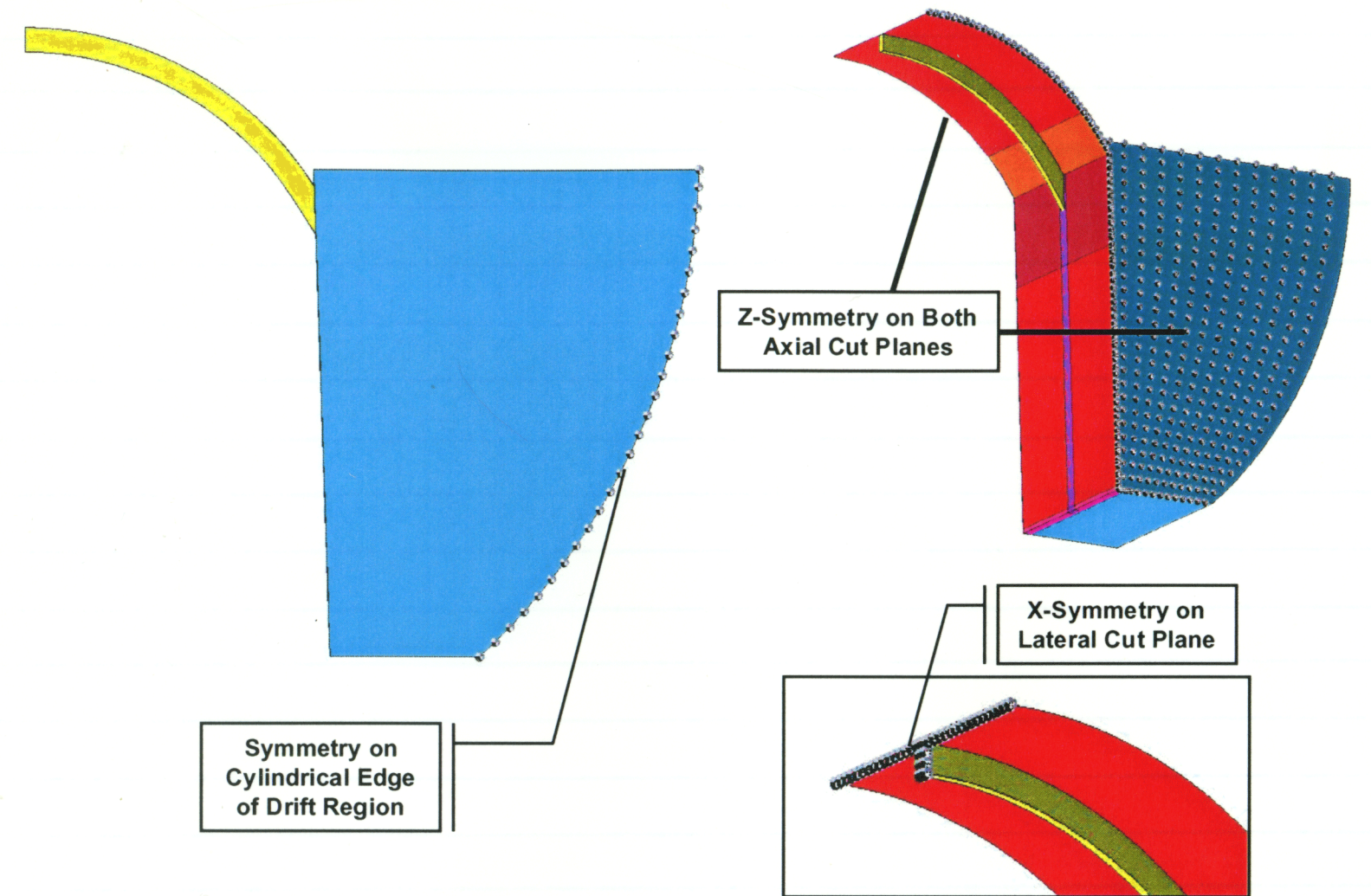
Analyses were performed using ABAQUS/Standard Version 5.8-16. Verification of this software is documented in the vendor's (Hibbitt, Karlsson & Sorensen, Inc.) quality program. The figures below illustrate the finite element model.



Overall, the drip shield mesh is identical to the modal analysis described previously except that symmetry conditions are used for this static analysis (see boundary conditions described below).

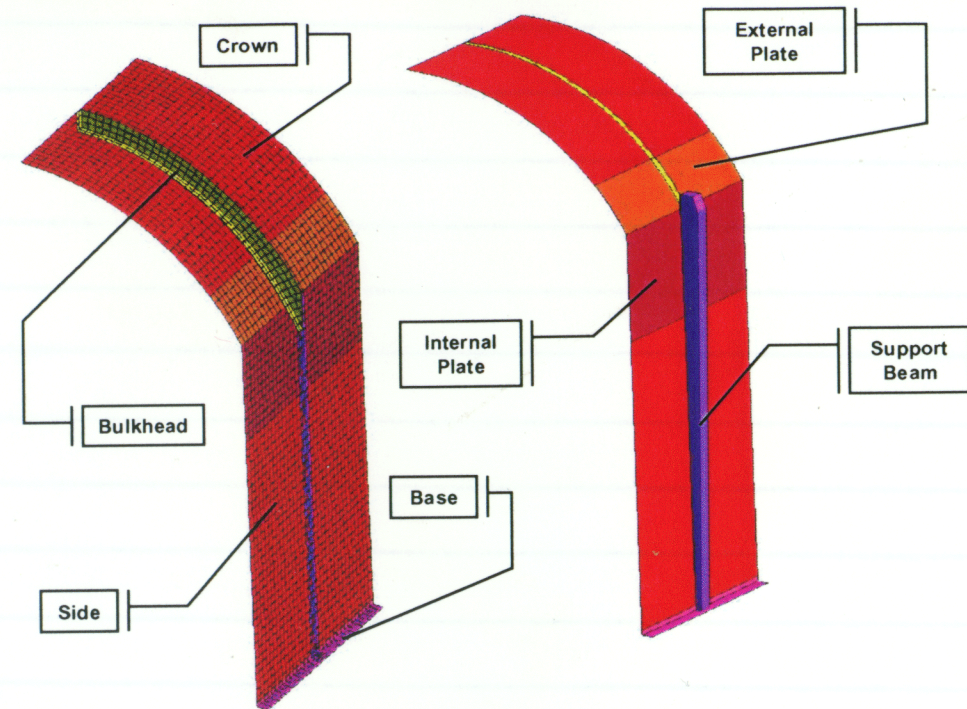
It was determined early in the analysis process that the side of the drip shield will need to interact with the accumulated rock. It is not sufficient to apply a static distribution of pressure down the side of the drip shield because this would allow large deflections of the drip shield side wall. The rock accumulated to the side of the drip shield, and trapped by the accumulated rock above, would clearly resist large deflections of the side wall. Therefore, the rock material interaction with the drip shield is simulated in two parts. The first part is a solid model of the rock material that interacts with the side of the drip shield through contact interaction elements. The top surface of this material is under pressure of the material above the modeled section. The second part is a distributed pressure load of the accumulated rock on the crown surface of the drip shield. These static rock pressure and crown pressure distributions are calculated based upon an elliptic drift collapse geometry. This is documented on p43 of scientific notebook 409 ("Repository Design and Thermal-Mechanics Effects") and the key formulas are programmed into the ABAQUS subroutine dload.f, which is archived with the electronic data.

The figure below illustrates the boundary conditions applied to the simulation. The resultant model simulates a symmetric accumulation of rockfall material in an elliptical drift collapse geometry condition. The drip shield is simulated as a structure that repeats continuously in the axial direction. This represents the middle section of a drip shield and is slightly conservative, as there is no benefit from the stiffer end structures of a drip shield segment.



Material properties for the drip shield components are identical to those for the drip shield model documented from page 80 of this scientific notebook. The table and figure below provides a cross reference to how those materials are assigned for the drip shield components of this model.

	Ti Grade7	Ti Grade24	Alloy 22
Crown	X		
Side	X		
Inner Plate	X		
Outer Plate	X		
Bulkhead		X	
Support Beam		X	
Base			X



The rockfall drift material was derived from two sources. First, Poisson's ratio is derived from the factor K_0 used to describe accumulated rock rubble load on p106 of this scientific notebook such that:

$$\nu = K_0 / (K_0 + 1)$$

Thus, at $K_0=0.2$ we find that $\nu=0.1667$. $K_0=0.2$ is assumed for the accumulated rock rubble discussed in scientific notebook 409 (p43).

A second source of data is used to estimate Young's Modulus. "Embankment-Dam Engineering", by Heirshfeld et al., 1973 provides insight into the behavior of several types of gravel and rockfill material through triaxial test data in Table 15 on p154. Stress and strain data from this table can be used to solve for Young's modulus using standard isotropic material relationships.

$$E = (\Delta s_1 - \nu(2\Delta s_3)) / \Delta e_1$$

where
 Δs_1 = change in radial stress
 Δs_3 = change in axial stress
 Δe_1 = change in radial strain
 ν = Poisson's ratio

The data in Heirshfeld et al. suggests a Young's modulus in the range of $3.0e+7$ Pa (two orders of magnitude greater than the parent rock block material used for impact analysis). It is possible that the actual rockfall material stiffness could be orders of magnitude stiffer or softer than $3.0e+07$. For this reason several simulations have been performed to characterize drip shield response with accumulated rockfall material of several modulus values shown. Values greater than $3.0e+07$ were not simulated because the results are trivial since the drip shield structure is stable at these stiffer assumptions.

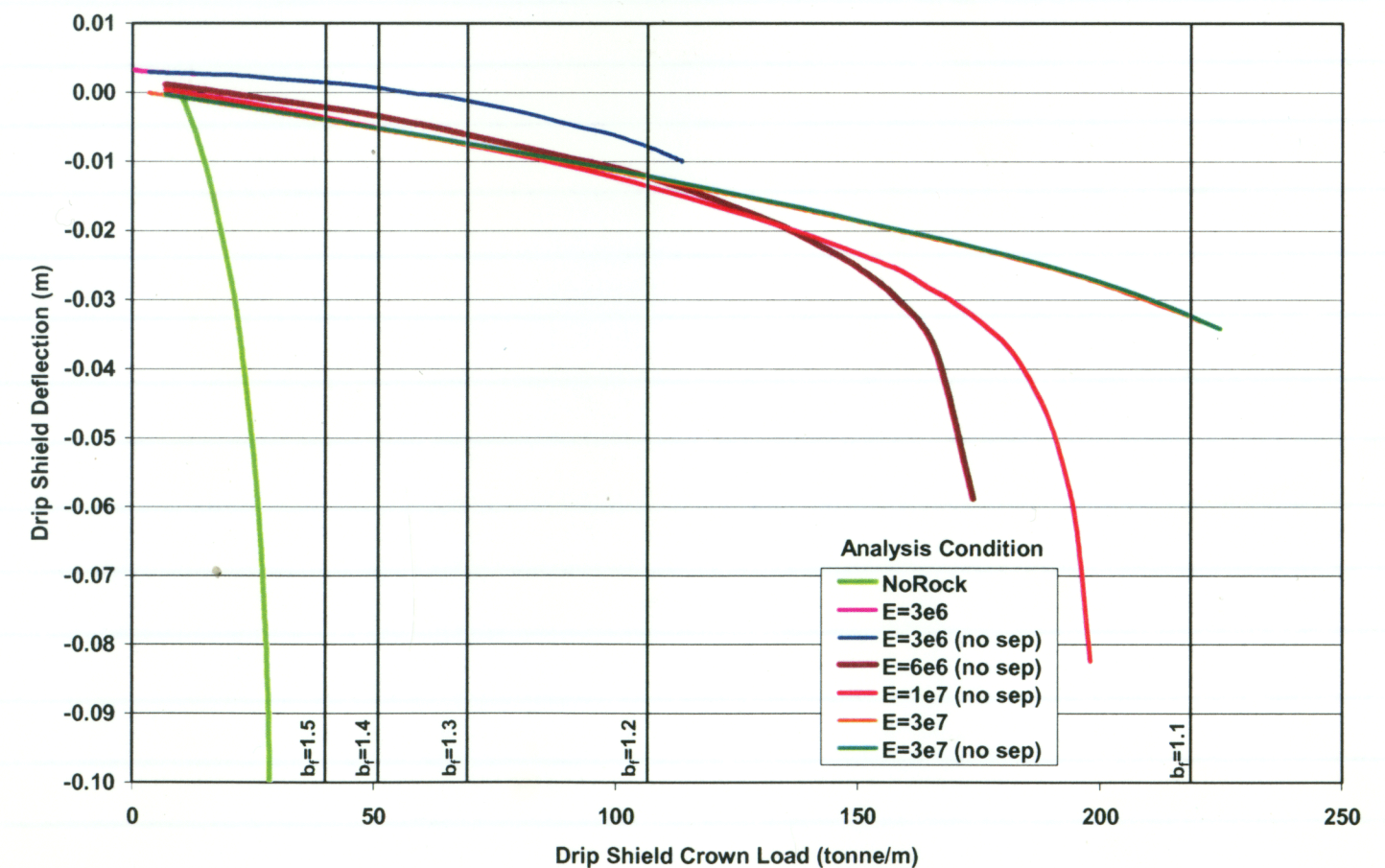
Simulation	Young's Modulus E (Pa)
1	no rock
2	$3.0e+06$
3	$6.0e+06$
4	$1.0e+07$
5	$3.0e+07$

14 Nov 2002
 2002 Nov 14

The finite element solution is setup as a non-linear static analysis where time is ramped from zero to 4.19 seconds. At 4.19 seconds the pressure returned from dload.f (described above) delivers values equivalent to a bulking factor of 1.1. The steps in the solution are described in the table below. Several solutions are performed to explore the various accumulated rock material properties. Simulations are run until the full load is applied or until unstable conditions are reached in the solution. The unstable condition is characterized by large deflections of the drip shield crown and yielding of the bulkhead and plate components. ABAQUS generally cuts back the solution step size until convergence cannot be achieved without reducing step size below the prescribed limit. In these simulations this limit was a time increment of $1.0e-5$.

Load Step	Bulking Factor	Max. Crown Pressure (MPa)	Rock Material Static Pressure (MPa)	Total Vertical Load (tonne/seg)
1	1.5	155,546	149,699	39.1
2	1.4	198,896	189,094	49.8
3	1.3	272,063	255,156	67.9
4	1.2	420,113	388,038	104.5
5	1.1	868,633	788,612	215.0

The basic message of the load versus deflection figure below is that the Drip Shield will collapse under lower bulking factors (b_f) as Young's modulus is reduced for the accumulated rockfall material. This is intuitive since a stiffer material will provide more support to buttress the Drip Shield. The figure also shows that the Drip Shield cannot support an accumulated rockfall load with a bulking factor greater than 1.2 if the modulus is less than $1.0e+07$ Pa. Also note that this figure shows many of the data lines with a "no sep" notation. This indicates that the simulated contact condition uses a no separation option. This option was perused because the full contact condition was unstable and it was not possible to estimate the collapse load because of chatter in the contact solution. However, the surfaces generally remained in contact. The no separation option was tested and proved to be robust and did not change the results. Note that there is no distinguishable difference between data of the same accumulated rockfall stiffness.



Five data abstractions were calculated to relate rock rubble vertical load to various drip shield consequences. Abstractions are based upon the methodology illustrated by the Mathcad sheet on page 94 and 95 of this scientific notebook. The first four are stress abstractions in two pairs. These abstractions find the accumulated load at which creep stress and yield stress is reached for the drip shield plate and bulkhead versus the assumed

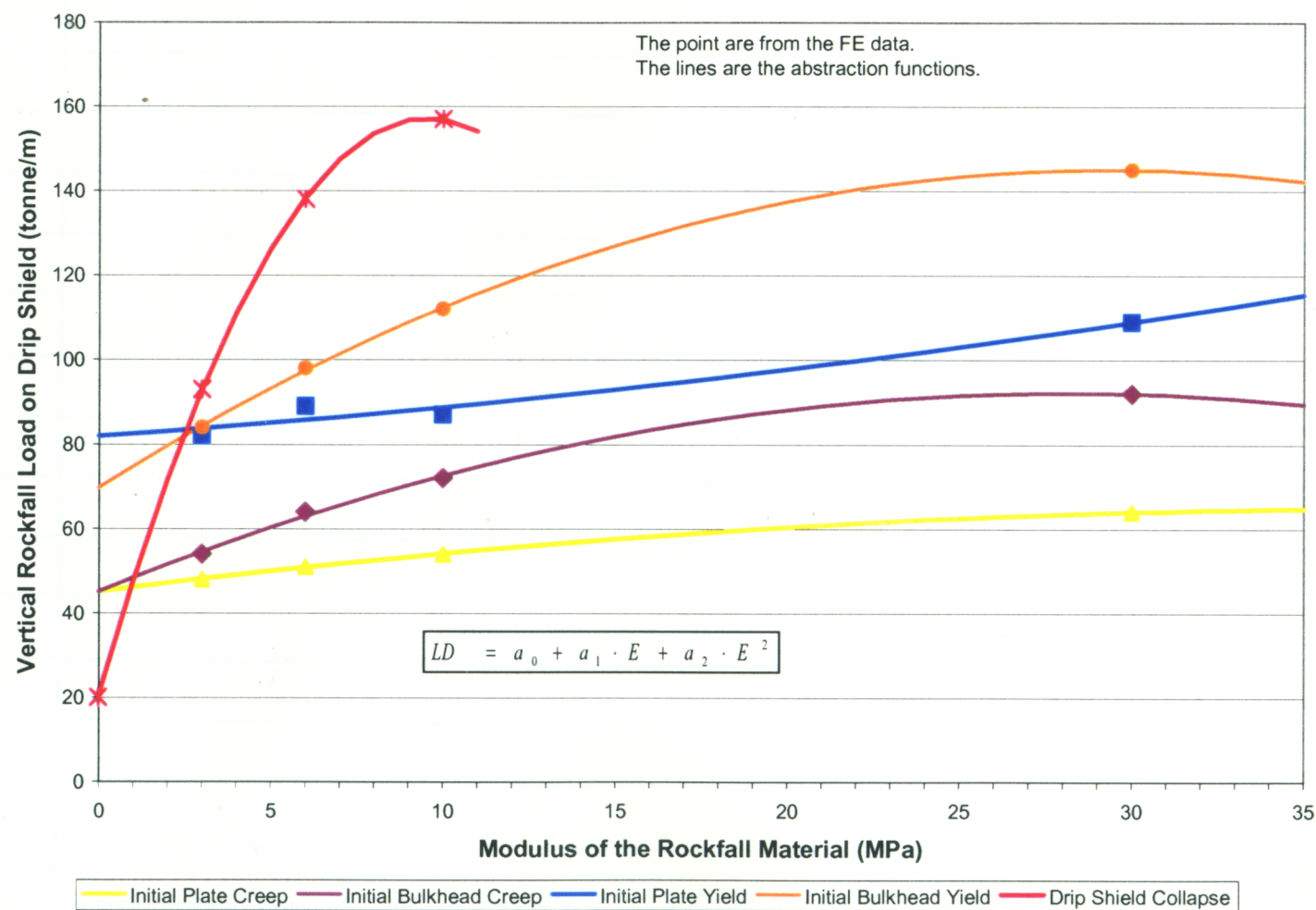
2002 Nov 14
 2002 Nov 14

stiffness of the rockfall material. The fifth abstraction finds the collapse load versus the assumed stiffness of the rockfall material. Collapse is assumed to be the load at the last converged iteration or where the maximum bulkhead stress begins to rise dramatically. There are no abstractions for plastic strain, deflection or stress in the support beam since the structure collapses before these values become significant. The table below summarizes the abstraction data.

Accumulated Rockfall Static Load Consequence Abstraction Data

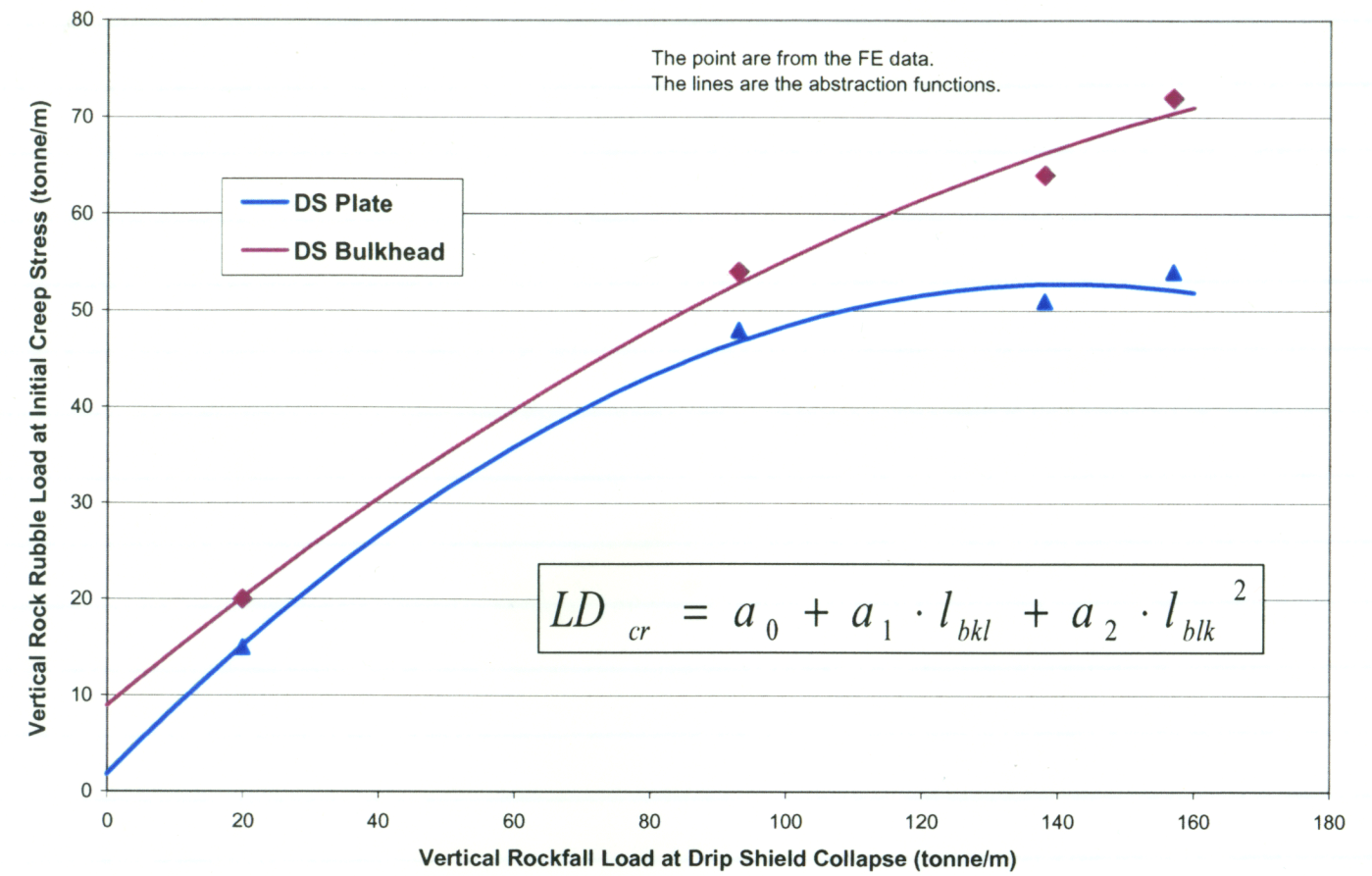
Simulation	Rockfall Modulus E (Pa)	Creep Stress Load		Yield Stress Load		Drip Shield Collapse Load
		Plate	Bulkhead	Plate	Bulkhead	
1	no rock	15	20	21	23	23
2	3.0e+06	48	54	82	84	95
3	6.0e+06	51	64	89	98	138
4	1.0e+07	54	72	87	112	157
5	3.0e+07	64	92	109	145	187
Abstraction coefficients	a0	4.51E+01	4.50E+01	8.19E+01	6.97E+01	2.01E+01
	a1	1.03E+00	3.34E+00	5.76E-01	5.14E+00	2.87E+01
	a2	-1.34E-02	-5.93E-02	1.09E-02	-8.77E-02	-1.50E+00

The figure below provides a summary of the abstractions. This includes abstraction data points from simulation, the abstraction formula and the abstraction curves for all five cases. Calculation sheets for all abstractions have been archived on CDROM.



Because of the uncertainty associated with the rock rubble material and thus its consequence on drip shield behavior an additional pair of data abstractions was calculated to relate the drip shield collapse load to the load where creep stress levels are reached for the plate and bulkhead. This abstraction may be used in the MECHFAIL code where a beta distribution can be defined for the buckling load of the drip shield. Given that load the abstraction presented below will predict the load at which creep begins for each component. The following table and figure summarize this abstraction.

Collapse Load	Load at First Plate Creep	Load at First Bulkhead Creep
20	15	20
93	48	54
138	51	64
157	54	72
Abstraction Coefficients	1.78E+00	8.94E+00
	7.21E-01	5.88E-01
	-2.55E-03	-1.25E-03



Electronic files have been archived to 8mm magnetic tape. All tapes are dated Oct 2002 and were written using the tar command from SunOS. The tape is labeled:

DS Accumulated Rockfall FEA
Archived: 04 Nov 2002 **Tape 1/1**

Archived data related to the previous data is archived in the following directories:

Directory	Description
K0 0.2/E=1e07	Models with rock rubble modulus of 1e07
K0 0.2/E=1e07	Models with rock rubble modulus of 1e07
K0 0.2/E=1e07	Models with rock rubble modulus of 1e07
K0 0.2/E=1e07	Models with rock rubble modulus of 1e07
K0 0.2/NoRock	DS under vertical load with no rubble interaction on side

Other directories have been archived on this tape and are for information purposed only. Additional data, including graphics and charts from post processing has been archived to a CDROM labeled:

DS Accumulated Rockfall FEA
HyperMesh Models, Graphics and
Misc. Results Data Files
Nov 2002

14 Nov 2002

14 Nov 2002

Assessment of the Revised Drip Shield Design

A revision of the drip shield design was provided as supplemental information in the DOE response to Key Technical Issue Agreement CLST.2.01. The specific DOE report documenting the materials of construction and component dimensions of the drip shield is

OCRWM M&O. Drip Shield Structural Response to Rock Fall.
 $\phi\phi\phi - \phi\phi C - SSE\phi - \phi\phi 3\phi\phi - \phi\phi\phi - \phi\phi A$. ENG. 20040405. 0019.
 Las Vegas, NV: OCRWM M&O, 2004.

To facilitate the development of an "engineering" model of the drip shield that can be used to approximate its response to accumulated rockfall rubble loads, under static and seismic conditions, detailed finite element models were used to quantify estimates of the effective rock rubble spring constants and moment-rotation relationships of the drip shield "side" and "crown" transition. The engineering modeling approach was chosen because, once the basic non-linear relationships have been characterized, it can approximate the response of the drip shield to the loads of interest in a timely and efficient manner. Detailed finite element models can accommodate the nonlinear material behavior and complex interactions between the drip shield and rockfall rubble in a single analysis. ^{DA 5/19/05} Although the finite element method provides the capability of accounting for all of the requisite nonlinearities simultaneously, the turn-around times for the computations are unacceptably long.

The objectives of the drip shield process level modeling effort are to approximate the following:

- The buckling loads of the drip shield for varying in-drift temperature conditions
- The accumulated rockfall rubble loads that will induce stress levels that are sufficient to cause or initiate creeping of the drip shield materials for varying in-drift temperature conditions

- The potential effects of degradation of the invert on drip shield structural integrity
- The approximate response of the drip shield to accumulated rockfall rubble loads during a seismic event

As was pointed out earlier, the finite element method will be used to develop the Moment-Rotation curve for the drip shield "side" and "crown" transition. This curve will be generated for three different temperatures, i.e., ^{DA 5/19/05} 150, 260, and 316 °C. Note that temperature affects the Moment-Rotation curve because the yield and ultimate strengths of the drip shield materials are functions of temperature as conveyed in the table below.

Temp.	Titanium Grade 7		Titanium Grade 5	
	*Yield Stress, S_y	*Ultimate Strength, S_u	†Yield Stress, S_y	†Ult. Strength, S_u
Information potentially subject to copyright protection was redacted from this location.				
The redacted material is from the information listed above.				

* ASME B&PV code, Section II, Part D, Tables Y-1 and U.
 † Room temperature reference value obtained from ASTM B265-98, temperature correction factor extracted from Figure S.4.1.1.1 of the "Military Handbook: Metallic Materials and Elements for Aerospace Vehicle Structures."

The ABAQUS/Standard finite element program that will be used to calculate the Moment-Rotation relationship requires the conversion of the engineering or nominal stress values listed in the table above be converted to true, or Cauchy, stress equivalents. Also, the engineering or nominal strain must be converted to its ^{DA 5/19/05} ~~nominal~~ logarithmic strain equivalent. To perform this conversion, however, the engineering strain corresponding to the ultimate strength is required. Unfortunately, qualified data for this parameter as a function of temperature is not readily available. As a result, the room temperature minimum elongation value prescribed by the ASTM B265-98 will be used. For Ti-7 a value of 0.20 will be used and, for Ti-5, a value of 0.1 will be used.